Chemosphere 353 (2024) 141590

Contents lists available at ScienceDirect

Chemosphere

journal homepage: www.elsevier.com/locate/chemosphere

Effects of $ZnWO_4$ nanoparticles on growth, photosynthesis, and biochemical parameters of the green microalga *Raphidocelis subcapitata*

Renan Castelhano Gebara [a,*], Cínthia Bruno de Abreu [a], Giseli Swerts Rocha [b], Adrislaine da Silva Mansano [c], Marcelo Assis [d], Ailton José Moreira [e], Mykaelli Andrade Santos [f], Thalles Maranesi Pereira [g], Luciano Sindra Virtuoso [g], Maria da Graça Gama Melão [c], Elson Longo [a]

[a] *Center for the Development of Functional Materials (CDMF), Universidade Federal de São Carlos (UFSCar), Rodovia Washington Luís, Km 235, 13565-905, São Carlos, SP, Brazil*
[b] *Universitat Rovira i Virgili, Escola Tècnica Superior d'Enginyeria Química, Departament d'Enginyeria Química, Av. Països Catalans, 26, 43007, Tarragona, Spain*
[c] *Department of Hydrobiology (DHb), Universidade Federal de São Carlos (UFSCar), Rodovia Washington Luís, Km 235, 13565-905, São Carlos, SP, Brazil*
[d] *Department of Analytical and Physical Chemistry, University Jaume I (UJI), Castelló, Spain*
[e] *Chemistry Institute of Araraquara, Universidade Estadual Paulista (UNESP), Araraquara, SP, Brazil*
[f] *Embrapa Pecuária Sudeste, P.O. Box 339, São Carlos, SP, 13560-970, Brazil*
[g] *Chemistry Institute, Universidade Federal de Alfenas (UNIFAL-MG), Gabriel Monteiro da Silva, 700, Centro, 37130-000, Alfenas, MG, Brazil*

HIGHLIGHTS

- $ZnWO_4$-NPs presented low free ion (Zn^{2+}) release.
- Cell parameters: 96h-IC50 was 23.34 mg L^{-1}; increased cell size and granularity.
- Decrease of Chl *a* fluorescence and carbohydrates; and increase of Chl *a* content.
- Efficiency loss of the photosystem II and of the oxygen evolving complex.
- Increased non-regulated energy dissipation; closure of reaction centers.

GRAPHICAL ABSTRACT

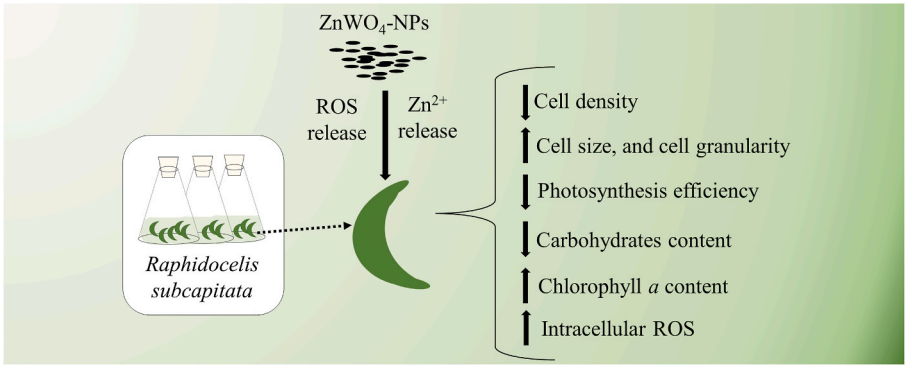

ARTICLE INFO

Handling editor: Maria Augustyniak

Keywords:
Chlorophyceae
Ecotoxicology
Physiology
Quenching

ABSTRACT

Nanoparticles have applications in many sectors in the society. $ZnWO_4$ nanoparticles ($ZnWO_4$-NPs) have potential in the fabrication of sensors, lasers, and batteries, and in environmental remediation. Thus, these NPs may reach aquatic ecosystems. However, we still do not know their effects on aquatic biota and, to our knowledge, this is the first study that evaluates the toxicity of $ZnWO_4$-NPs in a eukaryotic organism. We evaluated the toxicity of $ZnWO_4$-NPs on the green microalga *Raphidocelis subcapitata* for 96 h, in terms of growth, cell parameters, photosynthesis, and biochemical analysis. Results show that most of Zn was presented in its particulate form, with low amounts of Zn^{2+}, resulting in toxicity at higher levels. The growth was affected from 8.4 mg L^{-1},

* Corresponding author. Center for the Development of Functional Materials (CDMF), Universidade Federal de São Carlos (UFSCar), 13565-905, São Carlos, SP, Brazil.
E-mail address: nangebara@gmail.com (R.C. Gebara).

https://doi.org/10.1016/j.chemosphere.2024.141590
Received 20 December 2023; Received in revised form 8 February 2024; Accepted 29 February 2024
Available online 7 March 2024

Toxicity
$ZnWO_4$ nanoparticles

with 96h–IC50 of 23.34 mg L^{-1}. The chlorophyll *a* (Chl *a*) content increased at 30.2 mg L^{-1}, while the fluorescence of Chl *a* (FL3-H) decreased at 15.2 mg L^{-1}. We observed increased ROS levels at 44.4 mg L^{-1}. Regarding photosynthesis, the NPs affected the oxygen evolving complex (OEC) and the efficiency of the photosystem II at 22.9 mg L^{-1}. At 44.4 mg L^{-1} the qP decreased, indicating closure of reaction centers, probably affecting carbon assimilation, which explains the decay of carbohydrates. There was a decrease of qN (non-regulated energy dissipation, not used in photosynthesis), NPQ (regulated energy dissipation) and Y(NPQ) (regulated energy dissipation via heat), indicating damage to the photoprotection system; and an increase in Y(NO), which is the non-regulated energy dissipation via heat and fluorescence. The results showed that $ZnWO_4$-NPs can affect the growth and physiological and biochemical parameters of the chlorophycean *R. subcapitata*. Microalgae are the base of aquatic food chains, the toxicity of emerging contaminants on microalgae can affect entire ecosystems. Therefore, our study can provide some help for better protection of aquatic ecosystems.

1. Introduction

The global concern over the pollution of freshwater environments has escalated due to the increasing scarcity of potable water (Tortajada, 2020; Belhassan, 2021). The pollution of water bodies by metal, pesticides, pharmaceutics, dyes, and wastewater frequently affects the ecosystems biodiversity, besides making water unusable for human consumption (Harper et al., 2021). In addition to well-established sources of pollution, there is a rising concern about emerging contaminants, particularly nanoparticles (NPs), whose effects on aquatic biota need more investigation. NPs have widespread applications in various sectors, including the food industry, energy, medicine, agriculture, and environmental remediation (Dave and Chopda, 2014; Deshmukh et al., 2019; He et al., 2019; Assis et al., 2021). As nanotechnological product development continues to grow, these materials may be released into the environment, intentionally or inadvertently, during the production stage or at the end of their life cycle (Dwivedi et al., 2015; Abbas et al., 2020).

Among NPs, semiconductors (SCs) play a crucial role, showcasing electrical properties that lie between conductors and insulators. These materials are extensively employed due to their ability to generate photogenerated charge carriers, possessing unique chemical and physical properties. Notably, metal-based tungstate semiconductors exhibit a myriad of intriguing properties, including applications in electronics, catalysis, as well as antimicrobial and antitumoral activities (Karthiga et al., 2015; Assis et al., 2019; Cai et al., 2021). Despite the growing development of these materials, there is a scarcity of comprehensive studies exploring the toxicity effects of metal-based tungstates on aquatic organisms. Noteworthy is the finding that the SC α-Ag_2WO_4 demonstrates toxicity towards green algae due to the release of Ag^+, impacting growth and photosynthesis even at extremely low concentrations (Abreu et al., 2022a, 2022b). It demonstrates that metal-based tungstates may exert high toxicity on aquatic organisms.

Among metal-based tungstates, zinc tungstate ($ZnWO_4$) has garnered significant attention due to its vast potential applications, such as decontamination of organic compounds and metals in water, antibacterial activity, and used in the fabrication of sensors, lasers, and batteries (Huang et al., 2007; Shim et al., 2011; You et al., 2012; He et al., 2016, 2020; Ilango et al., 2018; Pereira et al., 2018; Li et al., 2019; Sivaganesh et al., 2020). Despite the numerous potential applications of $ZnWO_4$ nanoparticles ($ZnWO_4$-NPs), their toxicity has only been assessed for bacteria (antibacterial activity) (He et al., 2020), thus toxic effects of $ZnWO_4$-NPs on eukaryotic organisms are not described in literature. It is well established that zinc (Zn) is an essential metal to living organisms and abundant on Earth (Eisler, 1993; USGS, 2020). However, at concentrations higher than basal levels, Zn may exert toxicity on aquatic organisms (e.g. Wilde et al., 2006; Gebara et al., 2020; Gebara et al., 2021). Furthermore, zinc oxide nanoparticles (ZnO-NPs) may also cause deleterious effects on bacteria, algae, protozoa, crustaceans, nematodes, fish, and amphibians (Adam et al., 2015). In contrast, toxicity studies with tungsten (W) suggest that it exerts deleterious effects at high levels, such as 75% growth inhibition of the alga *Selenastrum capricornutum* at 2.42 g W L^{-1}; 48h-LC50 of 0.34 g W L^{-1} for the cladoceran *Daphnia magna*; and 4d-LD50 of 2.06 g W L^{-1} for the fish *Poecilia reticulate* (Strigul et al., 2009, 2010).

In this study, we evaluated the toxicity of $ZnWO_4$-NPs on the cosmopolitan green microalga *R. subcapitata* (previously known either as *Pseudokirchneriella subcapitata*, or *Selenastrum capricornutum*). The green microalga *R. subcapitata* is used worldwide in toxicity tests, being recommended as test organism in many international guidelines (USEPA, 2002; OECD, 2011). In addition to traditional algal growth inhibition tests, several studies emphasize the importance of assessing multiple endpoints, including physiological and biochemical parameters (e.g. Alho et al., 2020; Reis et al., 2022). It is known that metals, such as Zn, may affect the photosynthesis of *Raphidocelis subcapitata*, negatively impacting the efficiency of photosystem II (PSII) and the efficiency of the oxygen-evolving complex (OEC), respectively, at 0.03 and 0.005 mg Zn L^{-1}, after a 96 h exposure (Gebara et al., 2023). In this study, we assessed several parameters, including cell growth, cell size, cell granulometry, fluorescence of chlorophyll *a* (Chl *a*), production of reactive oxygen species (ROS), photosynthetic parameters (efficiency of PSII, efficiency of the OEC, photochemical and non-photochemical quenchings, and rapid light curves), Chl *a* content, and total carbohydrates. Additionally, we proposed a toxicity mechanism of $ZnWO_4$-NPs based on materials chemistry.

Since $ZnWO_4$-NPs may end up in aquatic environments mainly due to their applications in environmental remediation (He et al., 2020), it is crucial to assess their toxicity on aquatic organisms, such as microalgae, which are at the base of aquatic food webs, playing a crucial role in nitrogen fixation, oxygen production, and primary production in aquatic ecosystems (Chapman, 2010).

2. Material and methods

This section describes a summary of the material and methods. The detailed procedures are available in the supplementary material.

2.1. Nanoparticle: synthesis and characterization

The $ZnWO_4$-NPs were synthesized using the coprecipitation method followed by microwave hydrothermal irradiation. The structural characterization of the materials was conducted using a Rigaku XRD, model DMax2500PC. Scanning electron microscopy (SEM) images were obtained using a cold field emission microscope (JEOL model 7500F). The characterization of NPs in aqueous solutions (i.e., LC Oligo (algal medium) and ultrapure water) consisted in analysis of dynamic light scattering (DLS), polydispersity index (PdI), and zeta potential, using a Zetasizer Nano ZS90 (Malvern).

2.2. Algae culture and toxicity tests

The Chlorophyceae *Raphidocelis subcapitata* was cultured at pH 7.0 in LC Oligo medium (AFNOR, 1980), at 25 ± 2 °C, in a 12/12 h light/dark photoperiod (4200 lux). The composition of LC Oligo medium is presented in Table S1 (supplementary material). The medium was autoclaved (121 °C, 1 atm above standard pressure, 20 min) before use.

The 96 h toxicity tests were performed in polycarbonate flasks, filled with autoclaved LC Oligo medium (initial pH ≈ 7.0). The volume of medium did not exceed 50% of the flask volume. Based on preliminary ranging-finding tests, *R. subcapitata* was exposed to the concentrations of 0 (control), 8.45, 15.20, 22.87, 30.18 and 43.46 mg L^{-1} of total $ZnWO_4$, which corresponds to 0 (control), 0.04, 0.08, 0.15, 0.25 and 0.28 mg L^{-1} of dissolved Zn. The microalga at exponentially growing phase was inoculated at a concentration of 10^5 cells mL^{-1}, to obtain enough biomass for the biochemical analysis at the end of the toxicity test (Moreira et al., 2020; Reis et al., 2022). All parameters were evaluated in triplicate.

2.3. Flow cytometry: density, cellular parameters, and ROS production

The algal samples were analyzed in a FACSCalibur cytometer (Becton Dickinson, San Jose, EUA) according to standard procedures (Sarmento et al., 2008). We evaluated cell counting, cellular size (FSC–H), cellular granularity (SSC–H), and fluorescence of chlorophyll *a* (FL3-H). For ROS analyses, *in vivo* samples were incubated with 10 μM of DCFH-DA (2′7′-Dichlorofluorescein diacetate, CAS number 2044-85-1, Sigma Aldrich) (Hong et al., 2009) for 1 h in the dark. After that, samples were run in the cytometer, and relative ROS was calculated according to standard equations (Hong et al., 2009; Gebara et al., 2020).

2.4. Pulse-amplitude modulated (PAM) fluorometry

Samples were run in a Phytoplankton Fluorometer Analyzer equipped with an ED-101US/MP optic driver (Phyto-PAM, Heinz Walz GmbH, Germany). At 0, 24, 48, 72 and 96 h, algal samples (*in vivo*) were dark-adapted for 15 min prior to analysis. We calculated the efficiency of the OEC and the maximum efficiency PSII (ϕ_M), using parameters generated by the equipment and equations from literature (Kriedemann et al., 1985; Schreiber, 2004).

At 72 h of exposure, we assessed the photochemical (qP) and non-photochemical (qN, NPQ, Y(NPQ) and Y(NO)) quenchings, accordioning to literature (Bilger and Bjorkman, 1990; Maxwell and Johnson, 2000; Juneau et al., 2002; Klughammer and Schreiber, 2008). We also analyzed rapid light saturation curves according to Rocha et al. (2021), calculating the relative electron transport rate (rETR = ϕ_M' x PAR) (Ralph et al., 2002), fitting of the light saturation curve (Jassby and Platt, 1976), and calculating the relative maximum electron transport rate ($_rETR_{max}$), the slope (α) of the curve, and the saturating irradiance ($Ek = {}_rETR_{max}/\alpha$) (Rocha et al., 2021).

2.5. Biochemical analysis: chlorophyll a (Chl a) and carbohydrates

For Chl *a* analysis after 96 h, samples were filtered in cellulose ester membranes (0.45 μm of pore size, Millipore) and were extracted with dimethyl sulfoxide (DMSO) (Shoaf and Lium, 1976), and then run in a HACH DR500 spectrophotometer (HACH Company, Loveland, CO, USA) at 664 and 630 nm. The Chl *a* content was calculated according to Jeffrey and Humphrey (1975). To quantify the carbohydrates after 96 h, samples were centrifuged (4400 rpm, 10 min), extracted by phenol-sulphuric reaction (Liu et al., 1973), and then run in a spectrophotometer at 485 nm. Total carbohydrates were quantified using a calibration curve (Fig. S1) with dextrose anhydrous (Mallinckrodt Chemicals, USA).

2.6. Metal determination

Test-solution samples were filtered in cellulose acetate filters (0.45 μm pore size, Sartorius, Germany). The filters were stored in Teflon flasks and then digested using inverted aqua regia (3 M HNO_3/1 M HCl), according to Lombardi et al. (2002). The fraction retained in the filter was determined as particulate, while the filtered solutions were defined as dissolved fraction. Moreover, for some NPs concentrations, the filtered solutions were centrifuged (4400 rpm, 45min – Eppendorf 5702 R, Germany) in 3 kDa Amicon centrifugal filters (Merck Millipore, Ireland), being quantified as free ion concentrations (< 3 kDa) (Mansano et al., 2018; Abreu et al., 2022b).

We used two equipment for Zn quantification. For the atomic absorption spectrometry analysis, it was used a high-resolution molecular absorption spectrometer with continuous source [HR-CS MAS ContrAA 300 model (Analytik Jena, Jena, Germany)]; the limit of determination (LOD) was 0.003 mg L^{-1}, while the limit of quantification (LOQ) was 0.01 mg L^{-1}. We also measured the samples by inductively coupled plasma mass spectrometry (ICP-MS), using an Agilent 7800 ICP-MS (Agilent Technologies, Tokyo, Japan); the LOD was 0.002 mg L^{-1}, while LOQ was 0.006 mg L^{-1}.

2.7. Data analyses

For statistical analysis, first the normality (Shapiro-Wilk test) and variance (Levene test) of data were checked. Normal data were analyzed with one-way analysis of variance (ANOVA), followed by Dunnett's test. We analyzed non-normal data using Kruskal-Wallis's test, followed by Dunn's test. For the maximum efficiency of the photosystem II (PSII) only, statistical differences were determined using *t*-test. For all tests, $\alpha = 0.05$. The inhibition concentration (IC) values were calculated using logistic curves (available in supplementary material).

3. Results and discussion

3.1. Nanoparticles: characterization, metal determination and toxicity mechanism

To analyze the structural order at both long and short ranges, X-ray diffraction (XRD) and Raman spectroscopy analyses were conducted, respectively. Fig. 1A displays the diffractogram for $ZnWO_4$-NPs synthesized using the coprecipitation method followed by microwave irradiation. It is evident that $ZnWO_4$-NPs possess a monoclinic structure with P2/c space group, consistent with ICSD (Inorganic Crystal Structure Database) card No. 84540. No formation of secondary phases is observed, indicating high sample purity. In Fig. 1B, the Raman spectrum of the $ZnWO_4$-NPs sample reveals distinct modes related to [WO_6] clusters. Consistent with XRD analysis, no additional modes are observed, indicating the high purity of the sample. The morphology of $ZnWO_4$-NPs by SEM images is depicted in Fig. 1C, comprising nanorods with a maximum dimension of 23.8 ± 6.9 nm. A high degree of morphological homogeneity is evident across the samples.

The $ZnWO_4$-NPs characterization on aqueous solution showed aggregation and agglomeration on both ultrapure water and LC Oligo (Table S2, supplementary material), with higher level of aggregation and agglomeration in the algal medium. At the highest concentration of 44.4 mg L^{-1}, the average hydrodynamic size was 634.73 ± 26.89 and 1431.3 ± 148.36 nm in ultrapure water and LC Oligo, respectively. The polydispersity index at 44.4 mg L^{-1} was 0.55 ± 0.06 and 0.65 ± 0.15 in ultrapure water and LC Oligo, respectively. The zeta-potential was around −30.0 mV for ultrapure water, indicating moderate stability; for the algal medium, we found values between −17.50 ± 2.36 and −11.30 ± 0.50 mV, indicating that they are relatively stable, according to literature classification (Jeong and Shin, 2018). Regarding the determination of Zn in test solution by ICP-MS and HR-CS MAS (Table S3, Supplementary Material), the greater amounts of Zn remained as particulate metal, while lower amounts were available as dissolved fraction and free ions (Zn^{2+}). At the highest concentration of 44.4 mg L^{-1} of total $ZnWO_4$, there was only 0.28 mg L^{-1} of dissolved Zn, and 0.17 mg L^{-1} of Zn^{2+}. This explains the observed toxicity only at higher levels of $ZnWO_4$, since most metal was complexed, and not available in the algal medium.

To better understand the effects of $ZnWO_4$-NPs on *R. subcapitata*, comprehending its mechanism of action is essential. SCs in general are efficient in generating ROS, as the charge pairs produced can interact

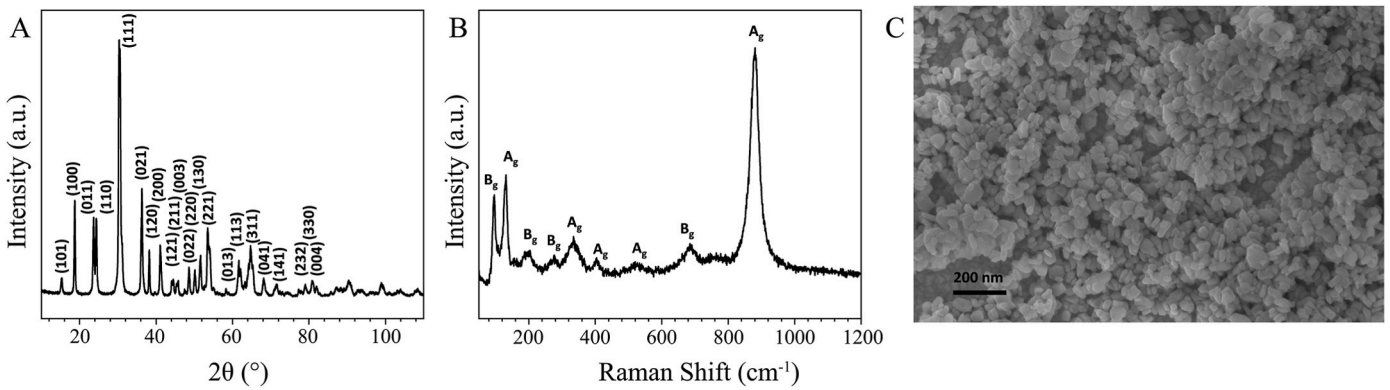

Fig. 1. X-ray diffraction (XRD) (A), Raman spectrum (B), and scanning electron microscopy (SEM) images (C) of the $ZnWO_4$ nanoparticles.

with molecules in their surroundings, especially H_2O and O_2. This process can occur in the dark due to electrons previously excited in their conduction band, but it is significantly amplified by light irradiation (Assis et al., 2023). Thus, the mechanism and toxicity of $ZnWO_4$-NPs involves not only the ionic release of their constituent components but may also be intrinsically connected to ROS production. What characterizes an SC, such as $ZnWO_4$, is the variation in its bandgap that can promote electrons to the forbidden region of the bandgap. This variation occurs on the surface of $ZnWO_4$-NPs due to structural defects and/or intrinsic oxygen vacancies (V_O) in the material (Fig. 2A (i)) (Pereira et al., 2018). These excited electrons control the activity of $ZnWO_4$, making it more or less effective for redox reactions on its surface. Initially, there is a transfer or absorption of electrons on the SC surface. In the case of $ZnWO_4$, each surface has a different bandgap, thus possessing different properties (Gouveia et al., 2018). The quantum parameter quantifying this is the charge density associated with the SC

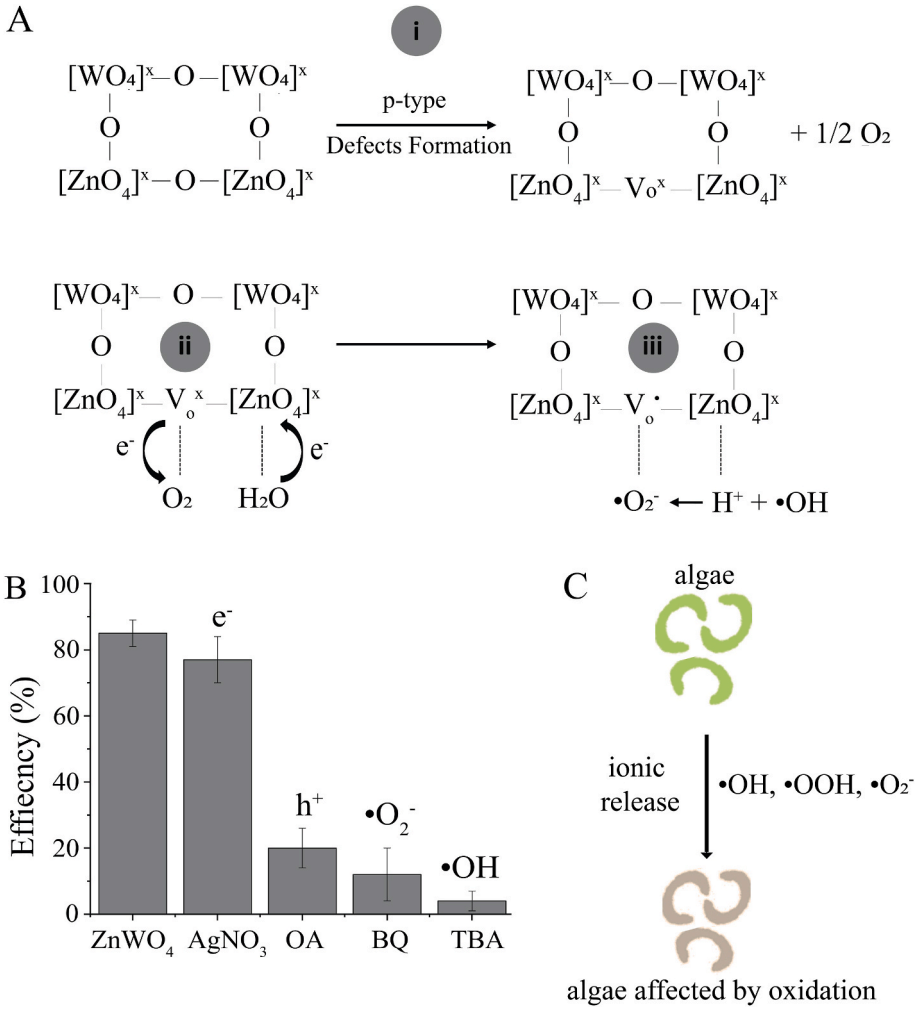

Fig. 2. Proposed ROS production by $ZnWO_4$ nanoparticles (A), and a test of free radical liberation, in which the decrease in photocatalytic efficiency was attributed to the presence of reactive species, as evidenced by the inhibition of the photocatalytic process (B). Mechanisms of activation leading to deleterious effects on *Raphidocelis subcapitata* by $ZnWO_4$-NPs (C).

region. In this way, the surface interaction of $ZnWO_4$ with O_2 and H_2O results in a molecular-level change in the bandgap when an electron is transferred from the conduction band by O_2 (Fig. 2A (ii)), forming the superoxide radical ($\bullet O_2^-$). This leads to a decrease in charge density in the conduction band and a transfer of electrons from the valence band to the conduction band to maintain neutrality. The creation of electron deficiency in the valence band promotes a new reaction with the H_2O molecule, breaking the hydrogen bond and promoting the formation of the hydroxyl radical ($\bullet OH$) and a proton (H^+) (Fig. 2A (iii)). This H^+ neutralizes the $\bullet O_2^-$, creating the hydroperoxyl radical ($\bullet OOH$) and returning the SC to its ground state. This mechanism is detailed in Fig. 2A and is consistent with the results of ROS generated in Fig. 2B, where a reduction in the photocatalytic efficiency in the decolorization of rhodamine B (RhB) is observed, especially when employing p-benzoquinone (BQ) and *tert*-butyl alcohol, which are scavengers of $\bullet O_2^-$ and $\bullet OH$, respectively (Tello et al., 2020; Libero et al., 2023). The effects of ROS generation, combined with the ionic release of the constitutive components of $ZnWO_4$, can lead to a series of impairments in the proper functioning of *R. subcapitata* (Fig. 2C). In algae exposed to Zn and ZnO-NPs, the oxidative stress caused by ROS may lead, for example, to lipidic peroxidation, damage to cell walls, cytotoxicity, and genotoxicity (Schiavo et al., 2016; Saxena and Harish, 2019; Filova et al., 2021).

3.2. Growth inhibition and cellular parameters

The daily growth (expressed as cell density) of *R. subcapitata* exposed to $ZnWO_4$-NPs is shown in Fig. 3A. After 24 h of exposure, the algal growth was significantly affected from 15.2 mg L^{-1} (Dunnett's test, $p < 0.05$), and after 96 h of exposure all treatments were affected compared to control (Dunnett's test, $p < 0.05$). At the highest concentration (44.4 mg L^{-1}), the algae grew around 4 times less than the control (Fig. 3A). The mean inhibition concentrations values were 96h-IC50 of 23.34 (21.12–25.56) mg L^{-1} and 96h-IC10 of 11.79 (8.95–14.63) mg L^{-1} (Table 1). However, it is important to note that these values correspond to the total amount of $ZnWO_4$-NPs. Around the IC50, at the intermediate concentration of 22.87 mg L^{-1} of total $ZnWO_4$-NPs, there was only 0.09 mg L^{-1} of Zn^{2+} (Table S3, supplementary material). Therefore, $ZnWO_4$-NPs presented very low free ions release (≈0.4% of Zn^{2+}) when compared to other metal-tungstates such as α-Ag_2WO_4, which released free silver (Ag^+) up to ≈ 30% of their total amount (Abreu et al., 2022b). Comparing to literature, Zn and ZnO-NPs presented IC-50 values on *R. subcapitata* of, respectively, 0.03 and 0.04 mg Zn L^{-1} (Aruoja et al., 2009; Gebara et al., 2020), far more toxic than $ZnWO_4$-NPs.

From the cytometer parameters, the relative cellular size (FSC–H) of algal cells increased at 44.4 mg L^{-1} from 24 h of exposure (Dunnett's test, $p < 0.05$), and after 96 h the cells increased in all treatments compared to controls (Dunnett's test, $p < 0.05$) (Fig. 3B). The relative cellular granularity (SSC–H) also increased with the increase of $ZnWO_4$-NPs concentration (Fig. 3C). Results show that SSC-H increased drastically in the first days of exposure, reaching around 2 times greater cell granularity at 44.4 mg L^{-1} than the controls, and this difference decayed to 1.2 times at the same concentration after 96 h (Fig. 3C). Regarding

Table 1
Growth inhibition (IC) concentration values (mg L^{-1}) of *Raphidocelis subcapitata* exposed to $ZnWO_4$ nanoparticles, after 96 h. The 95% confidence intervals are between brackets.

Test	96h-IC50	96h-IC20	96h-IC10
1	24.67 (22.45–26.89)	17.22 (14.32–20.13)	13.96 (10.74–17.17)
2	24.28 (22.06–26.49)	13.47 (11.08–15.86)	9.54 (7.23–11.86)
3	21.41 (19.40–23.42)	16.67 (13.83–19.51)	14.40 (11.12–17.67)
4	22.99 (20.55–25.43)	12.95 (10.31–15.58)	9.25 (6.70–11.81)
Mean	23.34 (21.12–25.56)	15.08 (12.39–17.77)	11.79 (8.95–14.63)

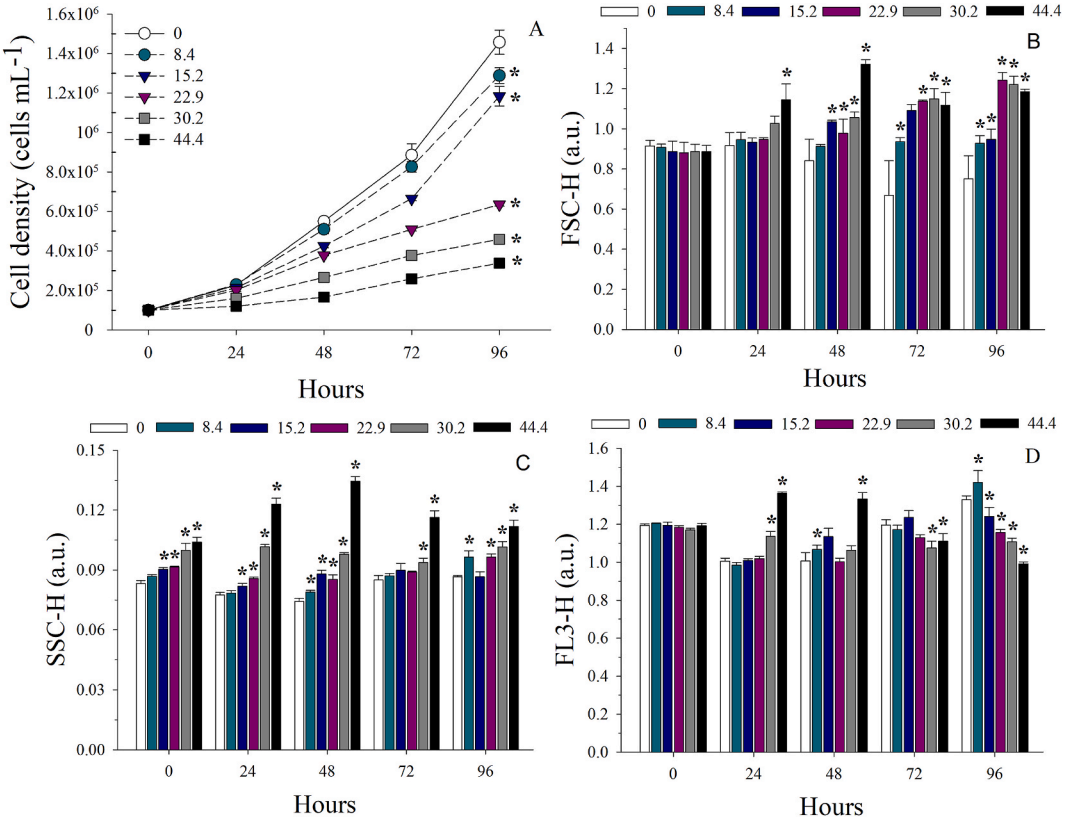

Fig. 3. Cell density (cells mL^{-1}) (A), cell size – FSC-H (B), cell granularity – SSC-H (C), and chlorophyll *a* fluorescence – FL3-H (D) of *Raphidocelis subcapitata* exposed to $ZnWO_4$ (mg L^{-1}) nanoparticles for 96 h. A.u. = arbitrary units. Asterisks represent statistical differences from control group (one-way ANOVA, Dunnett's test, $p < 0.05$).

FL3-H, it is notable an increasing trend on the fluorescence of Chl *a* the higher the NPs concentration, after 24 and 48 h of exposure (Fig. 3D); however, after 96 h FL3-H decreased significantly from 15.2 mg L^{-1} (Dunnett's test, $p < 0.05$). Corroborating our study, results from literature show that Zn and ZnO-NPs also increased FSC-H and SSC-H, and Zn decreased FL3-H of *R. subcapitata*, after 96h (Oukarroum et al., 2018; Gebara et al., 2020).

3.3. Physiology of the photosystem II (PSII)

From Fig. 4A, results show that $ZnWO_4$-NPs affected the ϕ_M of *R. subcapitata* at the highest concentrations from 48 h of exposure and, at 96 h of exposure, this parameter was affected from 22.9 mg L^{-1} (*t*-test, $p < 0.05$), i.e., the concentration around the 96h-IC50 regarding growth inhibition (Table 1). At the highest concentration of 44.4 mg L^{-1}, the ϕ_M decayed around 7% after 96 h (Fig. 4A). Results from literature regarding Zn toxicity on *R. subcapitata* also found a decrease of ϕ_M in concentrations of ≈0.16 mg L^{-1} (Machado et al., 2015) and 0.03 mg L^{-1} (Gebara et al., 2023), after a 72 h exposure. The efficiency of the OEC was affected since the beginning of the test from 30.2 mg L^{-1}, and from 22.9 mg L^{-1} after 96 h of exposure. It is known that there is a competition between Mn^{2+} (located in a cluster of the OEC) and Zn^{2+}, and that Zn^{2+} may substitute Mn^{2+}, disturbing the OEC (Rai et al., 2016; Souri et al., 2019). Conversely, toxicity results of *R. subcapitata* show that Zn affects the PSII after 72 h of exposure, decaying the efficiency of OEC and ϕ_M at 0.01 and 0.03 and mg L^{-1} Zn, respectively (Gebara et al., 2023).

From Fig. 5A, results show that the non-photochemical quenchings NPQ and Y(NPQ) decreased (Dunnett's test, $p < 0.05$) at 22.9 and 44.4 mg L^{-1}, indicating a damage to the regulated process of energy dissipation, which indicates the functioning of the photoprotection mechanism (Klughammer and Schreiber, 2008). At these treatments, there was also an increase in Y(NO), the non-regulated energy dissipation as heat and fluorescence (Klughammer and Schreiber, 2008). On the other hand, the photochemical quenching qP decayed only at 44.4 mg L^{-1} (Dunnett's test, $p < 0.05$) (Fig. 5A). The qP is related to the proportion of open reaction centers of PSII (Rocha et al., 2021), thus there was a closure of some reaction centers in this treatment, may affecting carbon assimilation (Krause and Jahns, 2003; Rocha and Espíndola, 2021). In our previous study of *R. subcapitata* exposed to Zn, we also found a decay of qN, NPQ and Y(NPQ) and an increase of Y(NO) at 0.01 mg Zn L^{-1} (Gebara et al., 2023). A study regarding cobalt toxicity on *R. subcapitata* showed that this essential metal also exerted damage to photoprotective mechanism of the alga (Rocha and Melão, 2024). According to rapid light curve results, the NPs affected the rETRmax only at 44.4 mg L^{-1} (Dunnett's test, $p < 0.05$) (Fig. 5B), indicating a decrease of the electron transport rate. Moreover, nor alpha (Fig. 5C) or Ek (Fig. 5D) changed statistically, i.e. the efficiency of light capture and saturation irradiance was not affected.

3.4. Biochemical parameters: chlorophyll a (Chl a) content, total carbohydrates, and reactive oxygen species (ROS) production

We observed an increment in Chl *a* content of almost 3 times, increasing from 0.27 pg Chl *a* $cell^{-1}$ in control groups to 0.75 pg Chl *a* $cell^{-1}$ at 44.4 mg L^{-1} (Fig. 6A). It is important to note that the Chl *a* content increased significantly at 30.2 and 44.4 mg L^{-1} (Dunnett's test, $p < 0.05$), i.e., concentrations in which the FL3-H decayed (Fig. 2D). It is known that the Zn^{2+} may replace the Mg^{2+} in chlorophyll molecules, turning them in unstable and less efficient chlorophylls (Souri et al., 2019). In this study, we hypothesize that the unstable and less efficient Chl *a* molecule presented lower fluorescence, demonstrated by the decay in FL3-H (Fig. 2D). Hence, there was an increase in Chl *a* molecule attempting to maintain the functioning of the PSII. Studies regarding effects of Zn and ZnO-NPs on algae reported a decrease of Chl *a* content (Saxena et al., 2021; El-Agawany and Kaamoush, 2023), but these results were reported as μg Chl *a* mL^{-1}. According to our data of Chl *a* in μg mL^{-1}, results show a trend to decrease (not significantly significant, $p > 0.05$) from 0.40 μg Chl *a* mL^{-1} in controls to 0.25 μg Chl *a* mL^{-1} at 44.4 mg L^{-1} (data not shown).

At 44.4 mg L^{-1} we noted a decrease of total carbohydrates (Fig. 6B), decaying from 2.30 in controls to 0.12 pg $cell^{-1}$ at 44.4 mg L^{-1} (Dunnett's test, $p < 0.05$). This result is in accordance to the decay of qP (Fig. 5A), indicating a closure of reaction centers, may resulting in lower carbon assimilation, and consequently lower carbohydrate content. Comparing to literature, Tripathi and Gaur (2006) also found a carbohydrate decrease in *Scenedesmus* sp. exposed to Zn. In algae, carbohydrates are biomolecules related to energy and carbon storage, and they act as a structural component of cell walls (Raven and Beardall, 2003; Markou et al., 2012). It is reported that ROS may destroy the carbohydrates and may damage the cell membranes (Liang et al., 2020). Therefore, it is in accordance to our data, since at 44.4 mg L^{-1} there was a decay of carbohydrates levels, and an increase of intracellular ROS (Fig. 6C); besides the free radicals that were liberated by $ZnWO_4$-NPs on algal medium (Fig. 2), may causing oxidative stress.

Regarding intercellular ROS production, results show a ROS decrease of 8% at the intermediate concentration of 22.9 mg L^{-1} (Dunnett's test, $p < 0.05$), and a ROS increase of 33% only at 44.4 mg L^{-1}(Dunnett's test, $p < 0.05$) (Fig. 6C). We suggest that antioxidant mechanisms of *R. subcapitata* were activated in response to $ZnWO_4$-NPs, therefore maintaining normal ROS levels at 8.4, 15.2, and 30.2 mg L^{-1}, and even may causing a decrease of ROS at the intermediate concentration of 22.9 mg L^{-1}. At 44.4 mg L^{-1} these antioxidant mechanisms were probably not enough to contain the increase of ROS levels. However,

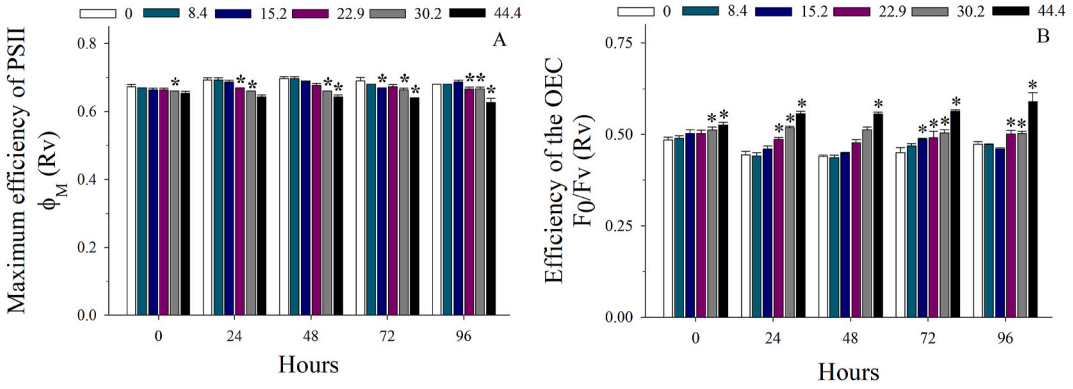

Fig. 4. Photosynthetic parameters of *Raphidocelis subcapitata* exposed to $ZnWO_4$ (mg L^{-1}) nanoparticles for 96 h. Panels (A): maximum efficiency of photosystems II (PSII) (Rv); (B): efficiency of the oxygen evolving complex (OEC), F_0/F_v (Rv). Asterisks represent statistical differences from control group (A: *t*-test, $p < 0.05$; B: one-way ANOVA, Dunnett's or Dunn's test, $p < 0.05$). Please note that: the higher the value of the F_0/F_v parameter, the lower the efficiency of the OEC.

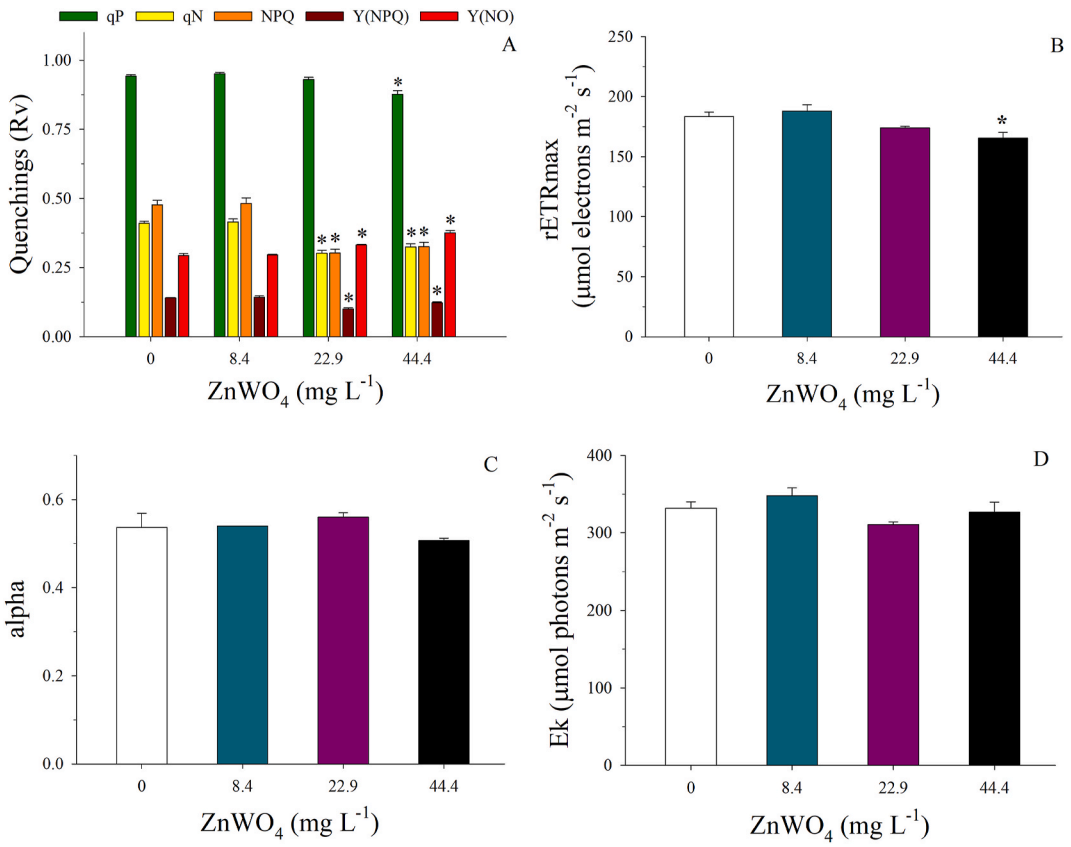

Fig. 5. Photosynthetic parameters of *Raphidocelis subcapitata* exposed to $ZnWO_4$ (mg L^{-1}) nanoparticles for 72 h. Panels (A): photochemical (qP) and non-photochemical (qN, NPQ, Y(NPQ), Y(NO)) quenchings; (B): relative maximum electron transport rate - rETRmax (µmol electrons m^{-2} s^{-1}); (C): alpha; (D): saturation irradiance – Ek (µmol electrons m^{-2} s^{-1}). Panels B–D refer to light curve parameters. Asterisks represent statistical differences from control group (one-way ANOVA, Dunnett's test, $p < 0.05$).

future studies measuring antioxidant enzymes are necessary to investigate this hypothesis. In studies with green algae exposed to Zn and ZnO-NPs, authors also observed ROS increase (Oukarroum et al., 2018; Gebara et al., 2023), in addition to the activation of antioxidant defenses (Hamed et al., 2017; Saxena et al., 2021).

4. Conclusion

Based on our results, the growth (expressed as cell density) was one of the most sensitive parameters after a 96h-exposure, affected from 8.4 mg L^{-1}, with a 96h-IC50 of 23.34 mg L^{-1}. Physiological analysis showed that $ZnWO_4$-NPs affected the OEC, consequently impairing the functioning of the PSII, decaying the ϕ_M. We observed a decrease of qP, indicating closure of reaction centers and probably resulting in lower carbon assimilation, explaining the observed decay of carbohydrates content. The qN, NPQ and Y(NPQ) quenchings decreased, suggesting a damage to photoprotection mechanisms; while Y(NO) increased, indicating an increase in non-regulated energy dissipation as heat and fluorescence. There was an increase of intracellular ROS only at the highest concentration, despite the free radicals liberated in the medium by $ZnWO_4$-NPs. The fluorescence of Chl *a* (FL3-H) decayed, which probably resulted in an increase of Chl *a* content to maintain the functioning of the PSII. Our study showed that $ZnWO_4$-NPs were toxic to the green alga *R. subcapitata* only at higher levels, since most of Zn was in its particulate form, with low Zn^{2+} levels. This is the first study regarding the toxicity of $ZnWO_4$-NPs on eukaryotic organisms. Our data reinforce the importance to assess the toxicity of emerging contaminants, with potential applications in many areas of the society on aquatic biota, particularly on microalgae, which are at the base of aquatic food webs of herbivory and, therefore, the impacts suffered by these primary producers can affect the entire ecosystem. This knowledge is essential to protect aquatic ecosystems.

CRediT authorship contribution statement

Renan Castelhano Gebara: Writing – review & editing, Writing – original draft, Project administration, Methodology, Investigation, Formal analysis, Data curation, Conceptualization. **Cínthia Bruno de Abreu:** Writing – review & editing, Methodology, Investigation, Formal analysis. **Giseli Swerts Rocha:** Writing – review & editing, Methodology, Formal analysis. **Adrislaine da Silva Mansano:** Writing – review & editing, Methodology, Formal analysis. **Marcelo Assis:** Writing – review & editing, Methodology, Investigation, Formal analysis, Data curation. **Ailton José Moreira:** Writing – review & editing, Investigation, Formal analysis. **Mykaelli Andrade Santos:** Writing – review & editing, Investigation, Formal analysis. **Thalles Maranesi Pereira:** Writing – review & editing, Investigation, Formal analysis. **Luciano Sindra Virtuoso:** Writing – review & editing, Investigation, Formal analysis. **Maria da Graça Gama Melão:** Writing – review & editing, Resources, Methodology, Conceptualization. **Elson Longo:** Writing – review & editing, Supervision, Resources, Methodology, Funding acquisition, Formal analysis.

Declaration of competing interest

The authors declare that they have no known competing financial interests or personal relationships that could have appeared to influence the work reported in this paper.

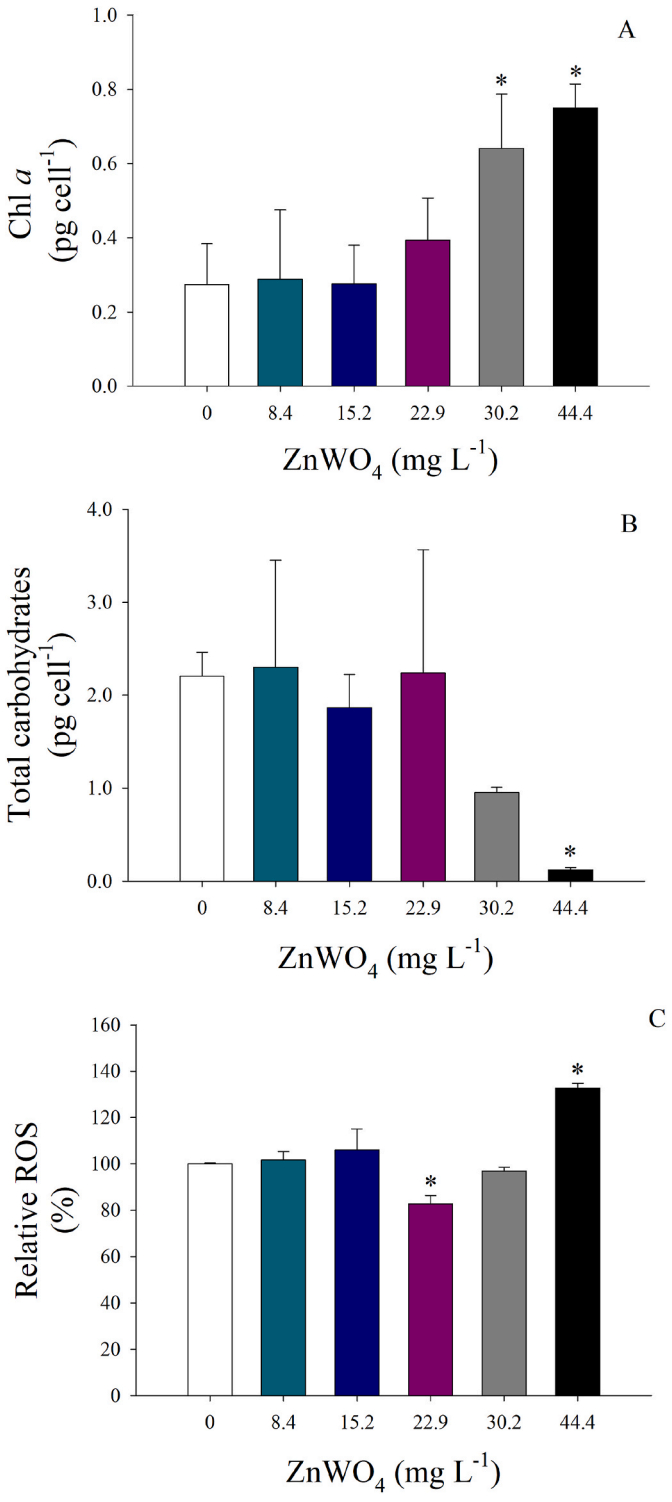

Fig. 6. Biochemical parameters of *Raphidocelis subcapitata* exposed to $ZnWO_4$ (mg L^{-1}) nanoparticles for 96h. Panels (A) Chlorophyll *a* (Chl *a*) (pg $cell^{-1}$); (B) total carbohydrates (pg $cell^{-1}$); and (C) relative reactive oxygen species (ROS) (%). Asterisks represent statistical differences from control group (one-way ANOVA, Dunnett's test, $p < 0.05$).

Data availability

Data will be made available on request.

Acknowledgements

This work was funded in part by the São Paulo Research Foundation - FAPESP, Brazil (grant ,2013/07296-2, 2014/14139-3 2018/07988-5, 2022/06219-3), (Financiadora de Estudos e Projetos - FINEP, Brazil), (Conselho Nacional de Desenvolvimento Científico e Tecnológico – CNPq, Brazil), and Coordenação de Aperfeiçoamento de Pessoal de Nível Superior - Brasil (CAPES, Brazil) – Finance Code 001. RCG and CBA have post-doctoral grants from the São Paulo Research Foundation - FAPESP (grant 2021/13583-0 and 2021/13607-7). M.A. was supported by the Margarita Salas postdoctoral, Spain contract MGS/2021/21 (UP2021–021) financed by the European Union-Next Generation EU. MGGM thanks the CNPq for the research productivity grant (process number 316064/2021-1). We are very thankful to Dr. Ana Rita de Araujo Nogueira for the help with the ICP-MS analysis; and to Dr. Ana Teresa Lombardi for the permission to use the Phyto-PAM fluorometer. We also would like to thank Dr. Hugo Sarmento for the permission to use the cytometer.

Appendix A. Supplementary data

Supplementary data to this article can be found online at https://doi.org/10.1016/j.chemosphere.2024.141590.

References

Abbas, Q., Yousaf, B., Amina Ali, M.U., Munir, M.A.M., El-Naggar, A., Rinklebe, J., Naushad, M., 2020. Transformation pathways and fate of engineered nanoparticles (ENPs) in distinct interactive environmental compartments: a review. Environ. Int. 138, 105646.

Abreu, C.B., Gebara, R.C., dos Reis, L.L., Rocha, G.S., Alho, L.O.G., Alvarenga, L.M., Virtuoso, L.S., Assis, M., Mansano, A.d.S., Longo, E., Melão, M.d.G.G., 2022a. Effects of α-Ag2WO4 crystals on photosynthetic efficiency and biomolecule composition of the algae *Raphidocelis subcapitata*. Water, Air, Soil Pollut. 233.

Abreu, C.B., Gebara, R.C., Reis, L.L.D., Rocha, G.S., Alho, L.O.G., Alvarenga, L.M., Virtuoso, L.S., Assis, M., Mansano, A.D.S., Longo, E., Melao, M., 2022b. Toxicity of alpha-Ag_2WO_4 microcrystals to freshwater microalga *Raphidocelis subcapitata* at cellular and population levels. Chemosphere 288, 132536.

Adam, N., Schmitt, C., De Bruyn, L., Knapen, D., Blust, R., 2015. Aquatic acute species sensitivity distributions of ZnO and CuO nanoparticles. Sci. Total Environ. 526, 233–242.

AFNOR, 1980. Norme experimentale. Essais deseaux Determination de I'nhibition de Scenedesmus subspicatus par une substance T90–T304. Paris.

Alho, L.O.G., Souza, J.P., Rocha, G.S., Mansano, A.D.S., Lombardi, A.T., Sarmento, H., Melao, M.G.G., 2020. Photosynthetic, morphological and biochemical biomarkers as tools to investigate copper oxide nanoparticle toxicity to a freshwater chlorophyceae. Environ. Pollut. 265, 114856.

Aruoja, V., Dubourguier, H.C., Kasemets, K., Kahru, A., 2009. Toxicity of nanoparticles of CuO, ZnO and TiO_2 to microalgae *Pseudokirchneriella subcapitata*. Sci. Total Environ. 407, 1461–1468.

Assis, M., Gouveia, A.F., Ribeiro, L.K., Ponce, M.A., Churio, M.S., Oliveira, O.N., Mascaro, L.H., Longo, E., Llusar, R., Guillamón, E., Andrés, J., 2023. Towards an efficient selective oxidation of sulfides to sulfones by NiWO and α-AgWO. Appl. Catal. Gen. 652.

Assis, M., Robeldo, T., Foggi, C.C., Kubo, A.M., Minguez-Vega, G., Condoncillo, E., Beltran-Mir, H., Torres-Mendieta, R., Andres, J., Oliva, M., Vergani, C.E., Barbugli, P. A., Camargo, E.R., Borra, R.C., Longo, E., 2019. Ag nanoparticles/alpha-Ag2WO4 composite formed by electron beam and femtosecond irradiation as potent antifungal and antitumor agents. Sci. Rep. 9, 9927.

Assis, M., Simoes, L.G.P., Tremiliosi, G.C., Coelho, D., Minozzi, D.T., Santos, R.I., Vilela, D.C.B., Santos, J.R.D., Ribeiro, L.K., Rosa, I.L.V., Mascaro, L.H., Andres, J., Longo, E., 2021. SiO2-Ag composite as a highly virucidal material: a roadmap that rapidly eliminates SARS-CoV-2. Nanomaterials 11, 1–19.

Belhassan, K., 2021. Water Scarcity Management. Water Safety, Security and Sustainability 443–462.

Bilger, W., Bjorkman, O., 1990. Role of the xanthophyll cycle in photoprotection elucidated by measurements of light-induced absorbance changes, fluorescence and photosynthesis in leaves of *Hedera canariensis*. Photosynth. Res. 25, 173–185.

Cai, Y., Yang, F., Wu, L., Shu, Y., Qu, G., Fakhri, A., Kumar Gupta, V., 2021. Hydrothermal-ultrasonic synthesis of CuO nanorods and CuWO4 nanoparticles for catalytic reduction, photocatalysis activity, and antibacterial properties. Mater. Chem. Phys. 258.

Chapman, R.L., 2010. Algae: the world's most important "plants"—an introduction. Mitig. Adapt. Strategies Glob. Change 18, 5–12.
Dave, P.N., Chopda, L.V., 2014. Application of iron oxide nanomaterials for the removal of heavy metals. Journal of Nanotechnology 2014, 1–14.
Deshmukh, S.P., Patil, S.M., Mullani, S.B., Delekar, S.D., 2019. Silver nanoparticles as an effective disinfectant: a review. Mater. Sci. Eng., C 97, 954–965.
Dwivedi, A.D., Dubey, S.P., Sillanpää, M., Kwon, Y.-N., Lee, C., Varma, R.S., 2015. Fate of engineered nanoparticles: implications in the environment. Coord. Chem. Rev. 287, 64–78.
Eisler, R., 1993. Zinc Hazards to Fish, Wildlife, and Invertebrates: A Synoptic Review. U. S. Department of the Interior Fish and Wildlife Service, Laurel, Maryland, p. 126.
El-Agawany, N.I., Kaamoush, M.I.A., 2023. Role of zinc as an essential microelement for algal growth and concerns about its potential environmental risks. Environ. Sci. Pollut. Control Ser. 30, 71900–71911.
Filova, A., Fargasova, A., Molnarova, M., 2021. Cu, Ni, and Zn effects on basic physiological and stress parameters of *Raphidocelis subcapitata* algae. Environ. Sci. Pollut. Res. Int. 28, 58426–58441.
Gebara, R.C., Alho, L.O.G., Abreu, C.B., Mansano, A.S., Moreira, R.A., Rocha, G.S., Melão, M.G.G., 2021. Toxicity and risk assessment of zinc and aluminum mixtures to *Ceriodaphnia silvestrii* (Crustacea: Cladocera). Environ. Toxicol. Chem. 40, 2912–2922.
Gebara, R.C., Alho, L.O.G., Mansano, A.D.S., Rocha, G.S., Melao, M., 2023. Single and combined effects of Zn and Al on photosystem II of the green microalgae *Raphidocelis subcapitata* assessed by pulse-amplitude modulated (PAM) fluorometry. Aquat. Toxicol. 254, 106369.
Gebara, R.C., Alho, L.O.G., Rocha, G.S., Mansano, A.S., Melão, M.G.G., 2020. Zinc and aluminum mixtures have synergic effects to the algae *Raphidocelis subcapitata* at environmental concentrations. Chemosphere 242, 125231.
Gouveia, A.F., Assis, M., S Cavalcante, L., Longo, E., Andrés, J., 2018. Reading at exposed surfaces: theoretical insights into photocatalytic activity of ZnWO4. Frontier Research Today 1.
Hamed, S.M., Zinta, G., Klock, G., Asard, H., Selim, S., AbdElgawad, H., 2017. Zinc-induced differential oxidative stress and antioxidant responses in *Chlorella sorokiniana* and *Scenedesmus acuminatus*. Ecotoxicol. Environ. Saf. 140, 256–263.
Harper, M., Mejbel, H.S., Longert, D., Abell, R., Beard, T.D., Bennett, J.R., Carlson, S.M., Darwall, W., Dell, A., Domisch, S., Dudgeon, D., Freyhof, J., Harrison, I., Hughes, K. A., Jähnig, S.C., Jeschke, J.M., Lansdown, R., Lintermans, M., Lynch, A.J., Meredith, H.M.R., Molur, S., Olden, J.D., Ormerod, S.J., Patricio, H., Reid, A.J., Schmidt-Kloiber, A., Thieme, M., Tickner, D., Turak, E., Weyl, O.L.F., Cooke, S.J., 2021. Twenty-five essential research questions to inform the protection and restoration of freshwater biodiversity. Aquat. Conserv. Mar. Freshw. Ecosyst. 31, 2632–2653.
He, G., Fan, H., Ma, L., Wang, K., Ding, D., Liu, C., Wang, Z., 2016. Synthesis, characterization and optical properties of nanostructured $ZnWO_4$. Mater. Sci. Semicond. Process. 41, 404–410.
He, H., Luo, Z., Tang, Z.-Y., Yu, C., 2019. Controllable construction of ZnWO4 nanostructure with enhanced performance for photosensitized Cr(VI) reduction. Appl. Surf. Sci. 490, 460–468.
He, H., Luo, Z., Yu, C., 2020. Multifunctional $ZnWO_4$ nanoparticles for photocatalytic removal of pollutants and disinfection of bacteria. J. Photochem. Photobiol. Chem. 401.
Hong, Y., Hu, H.Y., Xie, X., Sakoda, A., Sagehashi, M., Li, F.M., 2009. Gramine-induced growth inhibition, oxidative damage and antioxidant responses in freshwater cyanobacterium *Microcystis aeruginosa*. Aquat. Toxicol. 91, 262–269.
Huang, G., Zhang, C., Zhu, Y., 2007. ZnWO4 photocatalyst with high activity for degradation of organic contaminants. J. Alloys Compd. 432, 269–276.
Ilango, P.R., Prasanna, K., Jo, Y.N., Santhoshkumar, P., Lee, C.W., 2018. Wet chemical synthesis and characterization of nanocrystalline ZnWO4 for application in Li-ion batteries. Mater. Chem. Phys. 207, 367–372.
Jassby, A.D., Platt, T., 1976. Mathematical formulation of the relationship between photosynthesis and light for phytoplankton. Limnol. Oceanogr. 21, 540–547.
Jeffrey, S.W., Humphrey, G.F., 1975. New spectrophotometric equations for determining chlorophylls a, b, c1 and c2 in higher plants, algae and natural phytoplankton. Biochem. Physiol. Pflanz. (BPP) 167, 191–194.
Jeong, O., Shin, M., 2018. Preparation and stability of resistant starch nanoparticles, using acid hydrolysis and cross-linking of waxy rice starch. Food Chem. 256, 77–84.
Juneau, A., El Berdey, R., Popovic, P., 2002. PAM fluorometry in the determination of the sensitivity of *Chlorella vulgaris, Selenastrum capricornutum*, and *Chlamydomonas reinhardtii* to copper. Arch. Environ. Contam. Toxicol. 42, 155–164.
Karthiga, R., Kavitha, B., Rajarajan, M., Suganthi, A., 2015. Photocatalytic and antimicrobial activity of NiWO4 nanoparticles stabilized by the plant extract. Mater. Sci. Semicond. Process. 40, 123–129.
Klughammer, C., Schreiber, U., 2008. Complementary PS II quantum yields calculated from simple fluorescence parameters measured by PAM fluorometry and the saturation pulse method. PAM Appl Notes 1, 27–35.
Krause, G.H., Jahns, P., 2003. Pulse amplitude modulated chlorophyll fluorometry and its application in plant science. Light-Harvesting Antennas in Photosynthesis 373–399.
Kriedemann, P.E., Graham, R.D., Wiskich, J.T., 1985. Photosynthetic dysfunction and in vivo changes in chlorophyll *a* fluorescence from manganese-deficient wheat leaves. Aust. J. Agric. Res. 36, 157–169.
Li, M., Meng, Q., Li, S., Li, F., Zhu, Q., Kim, B.-N., Li, J.-G., 2019. Photoluminescent and photocatalytic ZnWO4 nanorods via controlled hydrothermal reaction. Ceram. Int. 45, 10746–10755.
Liang, S.X.T., Wong, L.S., Dhanapal, A.C.T.A., Djearamane, S., 2020. Toxicity of metals and metallic nanoparticles on nutritional properties of microalgae. Water, Air, Soil Pollut. 231.
Libero, L.O., Ribeiro, L.K., Granone, L.I., Churio, M.S., Souza, J.C., Mastelaro, V.R., Andrés, J., Longo, E., Mascaro, L.H., Assis, M., 2023. Introducing structural diversity: $Fe_2(MoO_4)_3$ immobilized in chitosan films as an efficient catalyst for the selective oxidation of sulfides to sulfones. ChemCatChem 15.
Liu, D., Wong, P.T.S., Dutka, B.J., 1973. Determination of carbohydrate in lake sediment by a modified phenol-sulfuric acid method. Water Res. 7, 741–746.
Lombardi, A.T., Vieira, A.A.H., Sartori, L.A., 2002. Mucilaginous capsule adsorption and intracellular uptake of copper by *Kirchneriella Aperta* (Chlorococcales). J. Phycol. 38, 332–337.
Machado, M.D., Lopes, A.R., Soares, E.V., 2015. Responses of the alga *Pseudokirchneriella subcapitata* to long-term exposure to metal stress. J. Hazard Mater. 296, 82–92.
Mansano, A.S., Souza, J.P., Cancino-Bernardi, J., Venturini, F.P., Marangoni, V.S., Zucolotto, V., 2018. Toxicity of copper oxide nanoparticles to Neotropical species *Ceriodaphnia silvestrii* and *Hyphessobrycon eques*. Environ. Pollut. 243, 723–733.
Markou, G., Angelidaki, I., Georgakakis, D., 2012. Microalgal carbohydrates: an overview of the factors influencing carbohydrates production, and of main bioconversion technologies for production of biofuels. Appl. Microbiol. Biotechnol. 96, 631–645.
Maxwell, K., Johnson, G.N., 2000. Chlorophyll fluorescence - a practical guide. J. Exp. Bot. 51, 659–668.
Moreira, R.A., Rocha, G.S., da Silva, L.C.M., Goulart, B.V., Montagner, C.C., Melao, M., Espindola, E.L.G., 2020. Exposure to environmental concentrations of fipronil and 2,4-D mixtures causes physiological, morphological and biochemical changes in *Raphidocelis subcapitata*. Ecotoxicol. Environ. Saf. 206, 111180.
OECD, 2011. OECD Guidelines for the Testing of Chemicals. Freshwater Alga and Cyanobacteria, Growth Inhibition Test, p. 25.
Oukarroum, A., Halimi, I., Siaj, M., 2018. Cellular responses of Chlorococcum sp. Algae exposed to zinc oxide nanoparticles by using flow cytometry. Water, Air, Soil Pollut. 230.
Pereira, P.F.S., Gouveia, A.F., Assis, M., de Oliveira, R.C., Pinatti, I.M., Penha, M., Goncalves, R.F., Gracia, L., Andres, J., Longo, E., 2018. ZnWO4 nanocrystals: synthesis, morphology, photoluminescence and photocatalytic properties. Phys. Chem. Chem. Phys. 20, 1923–1937.
Rai, R., Agrawal, M., Agrawal, S.B., 2016. Impact of heavy metals on physiological processes of plants: with special reference to photosynthetic system. In: Singh, A., Prasad, S., Singh, R. (Eds.), Plant Responses to Xenobiotics. Springer Nature, Singapore, pp. 127–140.
Ralph, P., Gademann, R., Larkum, A., Kühl, M., 2002. Spatial heterogeneity in active chlorophyll fluorescence and PSII activity of coral tissues. Mar. Biol. 141, 639–646.
Raven, J.A., Beardall, J., 2003. Carbohydrate metabolism and respiration in algae. In: Larkum, A.W.D., Douglas, S.E., Raven, J.A. (Eds.), Photosynthesis in Algae. Advances in Photosynthesis and Respiration. Springer, Dordrecht, pp. 205–224.
Reis, L.L., Alho, L.O.G., de Abreu, C.B., Gebara, R.C., Mansano, A.D.S., Melao, M.G.G., 2022. Effects of cadmium and cobalt mixtures on growth and photosynthesis of *Raphidocelis subcapitata* (Chlorophyceae). Aquat. Toxicol. 244, 106077.
Rocha, G.S., Espíndola, E.L.G., 2021. Copper affects photosynthetic parameters of N- or P-limited *Ankistrodesmus densus*. Environmental Advances 4.
Rocha, G.S., Melão, M.G.G., 2024. Does cobalt antagonize P limitation effects on photosynthetic parameters on the freshwater microalgae *Raphidocelis subcapitata* (Chlorophyceae), or does P limitation acclimation antagonize cobalt effects? More questions than answers. Environ. Pollut. 341, 122998.
Rocha, G.S., Parrish, C.C., Espíndola, E.L.G., 2021. Effects of copper on photosynthetic and physiological parameters of a freshwater microalga (Chlorophyceae). Algal Res. 54, 102223.
Sarmento, H., Unrein, F., Isumbisho, M., Stenuite, S., Gasol, J.M., Descy, J.-P., 2008. Abundance and distribution of picoplankton in tropical, oligotrophic Lake Kivu, eastern Africa. Freshw. Biol. 53, 756–771.
Saxena, P., Harish, 2019. Toxicity assessment of ZnO nanoparticles to freshwater microalgae *Coelastrella terrestris*. Environ. Sci. Pollut. Control Ser. 26, 26991–27001.
Saxena, P., Saharan, V., Baroliya, P.K., Gour, V.S., Rai, M.K., Harish, 2021. Mechanism of nanotoxicity in *Chlorella vulgaris* exposed to zinc and iron oxide. Toxicol Rep 8, 724–731.
Schiavo, S., Oliviero, M., Miglietta, M., Rametta, G., Manzo, S., 2016. Genotoxic and cytotoxic effects of ZnO nanoparticles for *Dunaliella tertiolecta* and comparison with SiO_2 and TiO_2 effects at population growth inhibition levels. Sci. Total Environ. 550, 619–627.
Schreiber, U., 2004. Pulse-Amplitude-modulation (PAM) fluorometry and saturation pulse method: an overview. In: Papageorgiou, G.C., Govindjee (Eds.), Chlorophyll *a* Fluorescence. Advances in Photosynthesis and Respiration. Springer, Dordrecht, pp. 279–319.
Shim, H.-W., Cho, I.-S., Hong, K.S., Lim, A.-H., Kim, D.-W., 2011. Wolframite-type ZnWO4 nanorods as new anodes for Li-ion batteries. J. Phys. Chem. C 115, 16228–16233.
Shoaf, W.T., Lium, B.W., 1976. Improved extraction of chlorophyll a and b from algae using dimethyl sulfoxide. Limnol. Oceanogr. 21, 926–928.
Sivaganesh, D., Saravanakumar, S., Sivakumar, V., Rajajeyaganthan, R., Arunpandian, M., Nandha Gopal, J., Thirumalaisamy, T.K., 2020. Surfactants-assisted synthesis of ZnWO4 nanostructures: a view on photocatalysis, photoluminescence and electron density distribution analysis. Mater. Char. 159.
Souri, Z., Cardoso, A.A., da-Silva, C.J., de Oliveira, L.M., Dari, B., Sihi, D., Karimi, N., 2019. Heavy metals and photosynthesis: recent developments. Photosynthesis, Productivity and Environmental Stress 107–134.

Strigul, N., Galdun, C., Vaccari, L., Ryan, T., Braida, W., Christodoulatos, C., 2009. Influence of speciation on tungsten toxicity. Desalination 248, 869–879.
Strigul, N., Koutsospyros, A., Christodoulatos, C., 2010. Tungsten speciation and toxicity: acute toxicity of mono- and poly-tungstates to fish. Ecotoxicol. Environ. Saf. 73, 164–171.
Tello, A.C.M., Assis, M., Menasce, R., Gouveia, A.F., Teodoro, V., Jacomaci, N., Zaghete, M.A., Andres, J., Marques, G.E., Teodoro, M.D., da Silva, A.B.F., Bettini, J., Longo, E., 2020. Microwave-driven hexagonal-to-monoclinic transition in BiPO4: an in-depth experimental investigation and first-principles study. Inorg. Chem. 59, 7453–7468.
Tortajada, C., 2020. Contributions of Recycled Wastewater to Clean Water and Sanitation Sustainable Development Goals. Npj Clean Water 3.
Tripathi, B.N., Gaur, J.P., 2006. Physiological behavior of *Scenedesmus* sp. during exposure to elevated levels of Cu and Zn and after withdrawal of metal stress. Protoplasma 229, 1–9.
USEPA, 2002. Short-term Methods for Estimating the Chronic Toxicity of Effluents and Receiving Waters to Freshwater Organisms 335. Washington, DC.
USGS, 2020. Mineral commodity summaries 2020: U.S. Geological Survey, 200 p., https://doi.org/10.3133/mcs2020.
Wilde, K.L., Stauber, J.L., Markich, S.J., Franklin, N.M., Brown, P.L., 2006. The effect of pH on the uptake and toxicity of copper and zinc in a tropical freshwater alga (*Chlorella* sp.). Arch. Environ. Contam. Toxicol. 51, 174–185.
You, L., Cao, Y., Sun, Y.F., Sun, P., Zhang, T., Du, Y., Lu, G.Y., 2012. Humidity sensing properties of nanocrystalline ZnWO4 with porous structures. Sensor. Actuator. B Chem. 161, 799–804.